Jimmy Miller
UC Davis
1/31/2016

Observing Epitaxial Growth, Structural Phases, and Structural Phase Transitions of Au on Ge (110) Using Low-Energy Electron Microscopy

Abstract:

The epitaxial growth, structural phases, and structural phase transitions of Au on Ge(110) were observed using low-energy electron microscopy. Live video data were recorded in real space as well as in reciprocal space at various temperatures and coverages. Au islands were found to grow fastest along one direction. The island shape could be controlled by adjusting the deposition temperature. Solid gold islands began diffusing across the surface once a critical temperature of around 750° C was reached. A surface phase transition was found around 450° C.

Introduction:

Attempting to control the structure of solid surfaces with multiple components requires an understanding of how the surface orders upon the adsorption of atoms. An understanding of the growth and nucleation of metal on elemental semiconductors is important due to its relevance to the formation of electrical contacts. Gold is a common metal used for electrical contacts on germanium semiconductor devices. Low-energy electron microscopy (LEEM) was used to study Au/Ge interfaces. The low-energy electron microscope chamber is connected to several other ultrahigh vacuum chambers which house an x-ray photoemission spectrometer (XPS) and a scanning tunneling microscope (STM) (Fig. 1,2). Magnetically coupled transfer rods are used to transfer samples from chamber to chamber. The rods can lock on to and release the sample holder via a mechanical spring-loaded mechanism. The sample holder (Fig. 3) was designed to keep the filament, used for electron-beam heating, electrically isolated from the sample. The contact pads at the bottom of the sample holder allow us to make

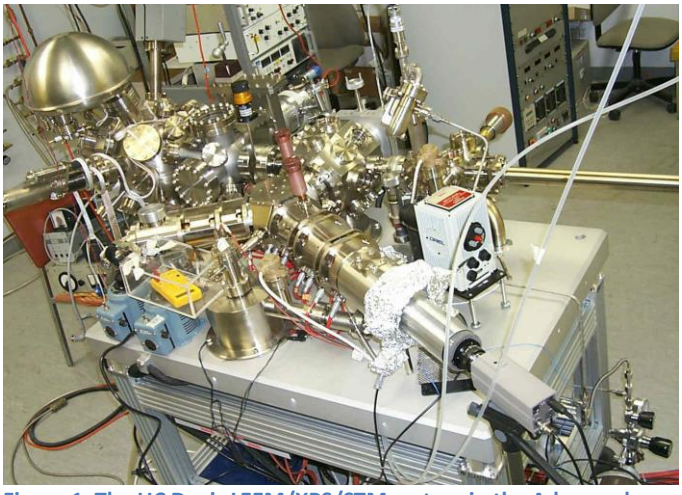

Figure 1: The UC Davis LEEM/XPS/STM system in the Advanced Surface Microscopy Facility

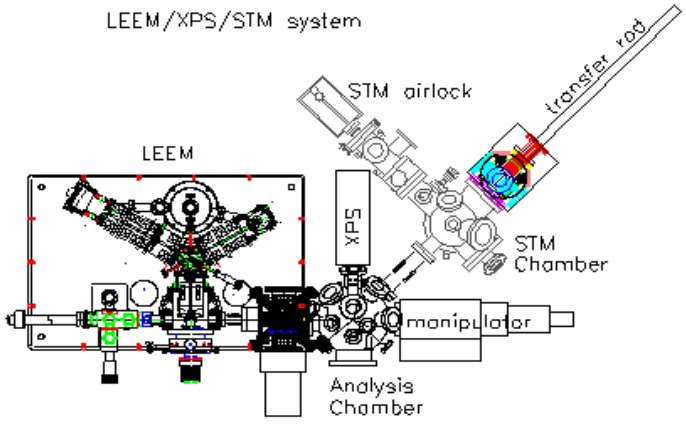

Figure 2: Diagram of the LEEM/XPS/STM system

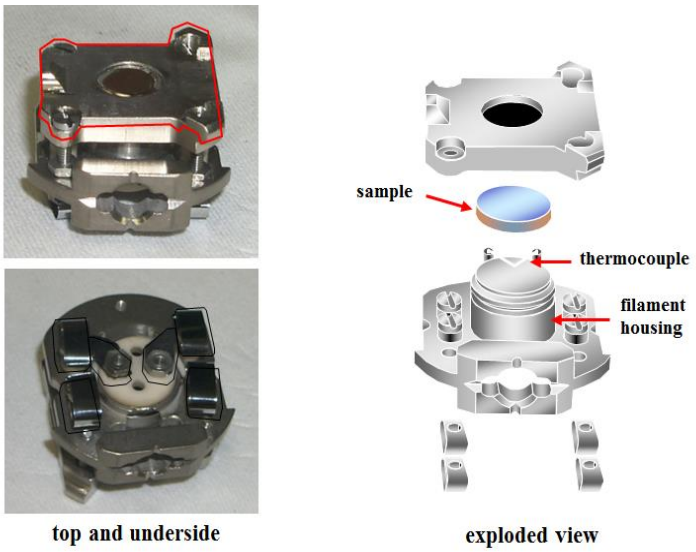

Figure 3: Sample holder features

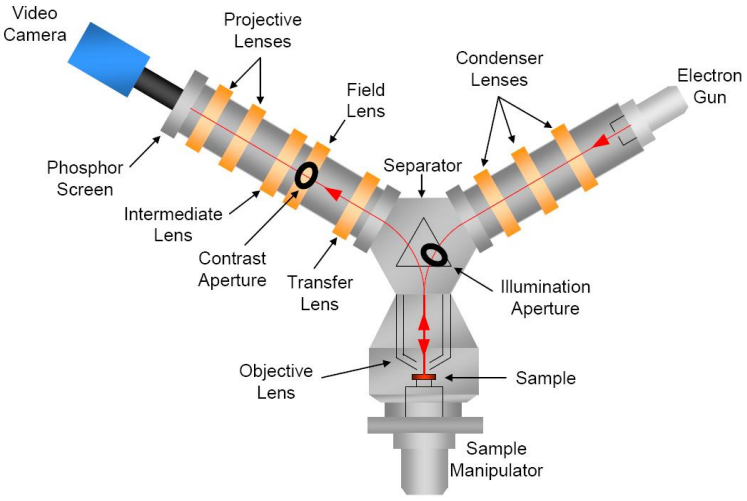

Figure 5: Diagram of the UC Davis Elmitec LEEM III

electrical connections in order to control and measure the filament current and the temperature of the sample. The voltage difference between the chromel and alumel wires is proportional to the sample's temperature. The low-energy electron microscope (Fig. 4) uses an electron gun with a lanthanum hexaboride cathode tip. Thermionic emission of electrons is achieved when current is driven through the tip which is held at -20 kV. The condenser lenses are held at ground. This potential difference creates a strong electric field that accelerates the electrons to 20 KeV by the time they have reached the objective lens. The sample is also held at -20 kV. This causes the electrons to decelerate quickly to a very low energy (1-100 eV). Such low energy electrons have a very short mean free path in materials making them surface sensitive. The magnetic beam separator directs the incoming beam towards the sample and directs the reflected beam towards the imaging optics.

In the bulk, germanium has a diamond cubic structure. At the surface the extra dangling bonds lead to a more complex, reconstructed structure. The two surface reconstructions on clean Ge(110) at room temperature are the (16x2) and the c(8x10) structures (Fig. 5). Scanning tunneling microscope

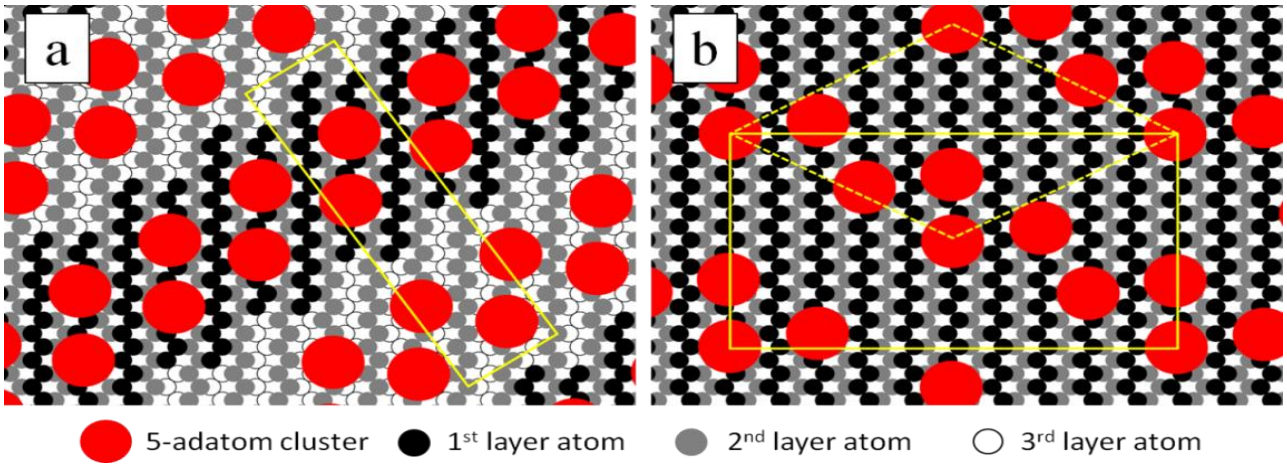

Figure 4: The atomic structure of clean germanium consists of both the (16x2) and c(8x10) phases. The (16x2) phase is seen on the left and the c(8x10) is on the right.

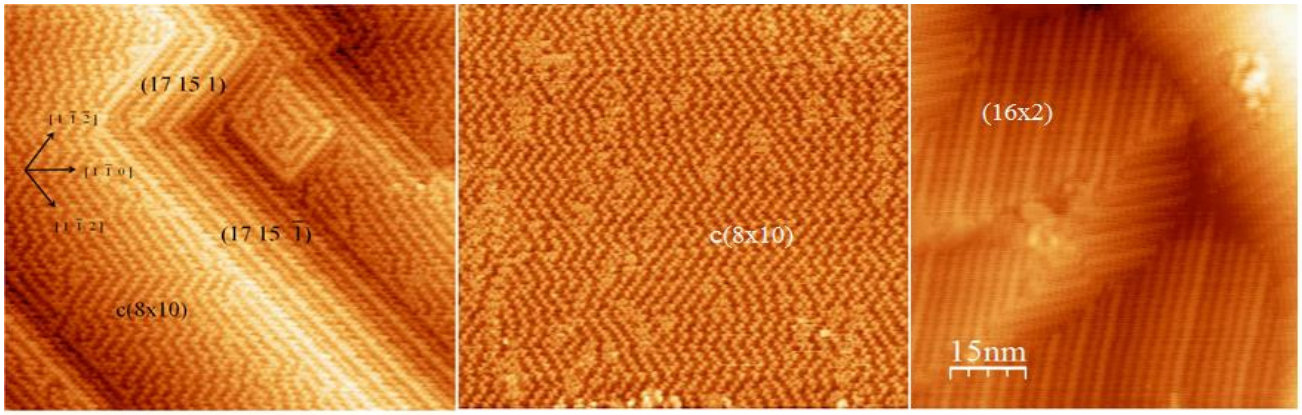

Figure 6: Scanning tunneling microscope images of clean Ge (110). The sample was annealed above 430°C and cooled resulting in c(8x10) and 16x2 reconstructions with [17 15 1] faceting. The sample voltage was -2.0 V and the tunneling current was 0.5 nA. The first two images are 100 nm x 100 nm.

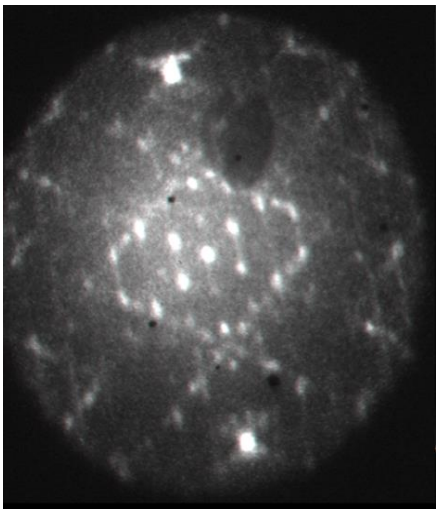

Figure 7: Diffraction image reveals patterns from both the (16x2) and the c(8x10) phases of Ge(110) superposed at room temperature ; sample must be cleaned through several cycles of sputtering and annealing before these reconstructed diffraction patterns are visible.

images of clean Ge(110) show the periodicity of the atomic structure (Fig. 6). Each phase has a unique diffraction patterns. We use low-energy electrons ranging from 1-100 eV (corresponding to a wavelength of 1-10 angstroms) in order to interact with surface atoms. Electron diffraction occurs because the wavelength of the electron is about the same size as the atomic spacing, similar to light interacting with a slit about the width of its wavelength.

The characteristic diffraction patterns from both the (16x2) and c(8x10) phases of Ge(110) are superposed at room temperature when we use low-energy electron diffraction to project the reciprocal space image of the surface formed at the back focal plane of the objective lens, onto the phosphor screen (Fig. 7). The reciprocal space image is formed at the back focal point of the objective lens. This reciprocal space plane is then projected to the phosphor screen. By adjusting the currents in the transfer, field, intermediate, and projective lenses, either the real space image or the reciprocal space image can be projected onto the phosphor screen. The computer controls allow us to switch from low-energy electron diffraction (LEED) imaging to real space imaging (LEEM) quickly. We use a contrast aperture to allow electrons from only a single diffraction spot to pass through to the screen when switching from LEED to LEEM. Bright-field imaging occurs when the central

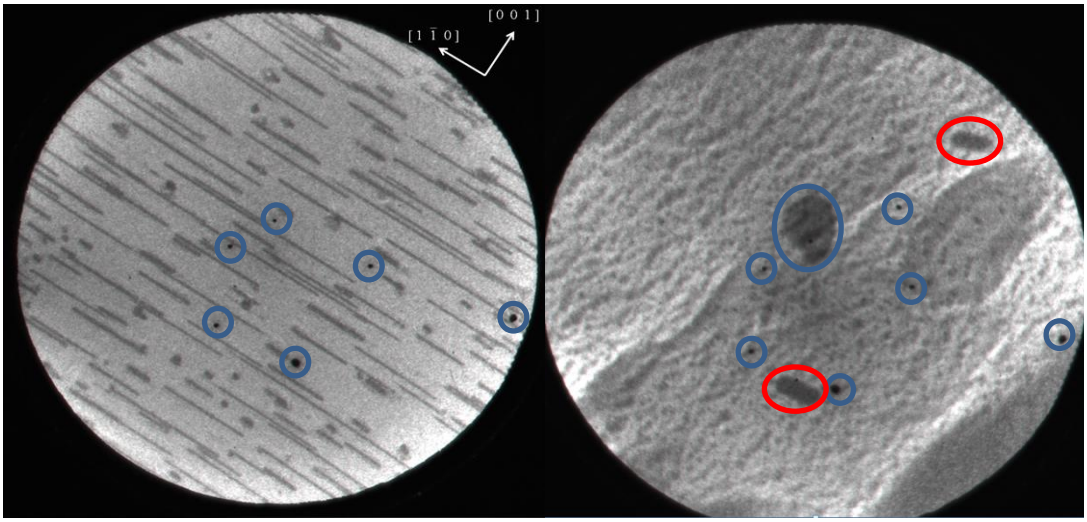

Figure 8a and 8b: One dimensional islands of Ag (left) and Au (right) on Ge(110) ; 10 µm field of view (FOV) The field of view is a measure of the diameter of the circular image created by the low-energy electron microscope. Channel plate defects are circled in blue while gold islands are circled in red.

electron diffraction spot (0,0) is selected with the contrast aperture in LEED mode before switching to LEEM. Differences in atomic structure lead to electron wave interference resulting in vertical diffraction contrast in bright-field images. Dark-field imaging occurs when the contrast aperture is adjusted so that it selects a diffraction spot other than (0,0) central spot. Contrast in dark-field images is a result of certain atomic structures on the surface diffracting while other structures may not diffract to the same spot.

LEEM/LEED Data:

Ag/Ge(110) interfaces were investigated previously by our research group. (Mullet thesis) (Fig. 8). The LEEM image in Figure 8a shows 7.6 ML of Ag that was deposited with the sample held at 460°C. The island growth is very one dimensional, with the preferred axis along the [1-1 0] direction. The LEEM image in Figure 8b shows 1 ML of Au that was deposited on a sample held at 690°C. The Au island growth also favors one direction. However, the Au islands are much wider. After this sample was dosed, we heated it to 815° C and then cooled it to around 500° C. The gold seems to have collected to the right side of the marked island. The outline of the islands shape remains (Fig. 9). At lower start voltages atomic steps are visible on the surface because of interference between the electron wavelengths. As the start voltage increases, the electron energy increases, which means the wavelength is much smaller. Smaller wavelengths can probe smaller surface features. This explains why the tiny pits in Figure 9 are visible when the start voltage is higher but invisible at lower values.

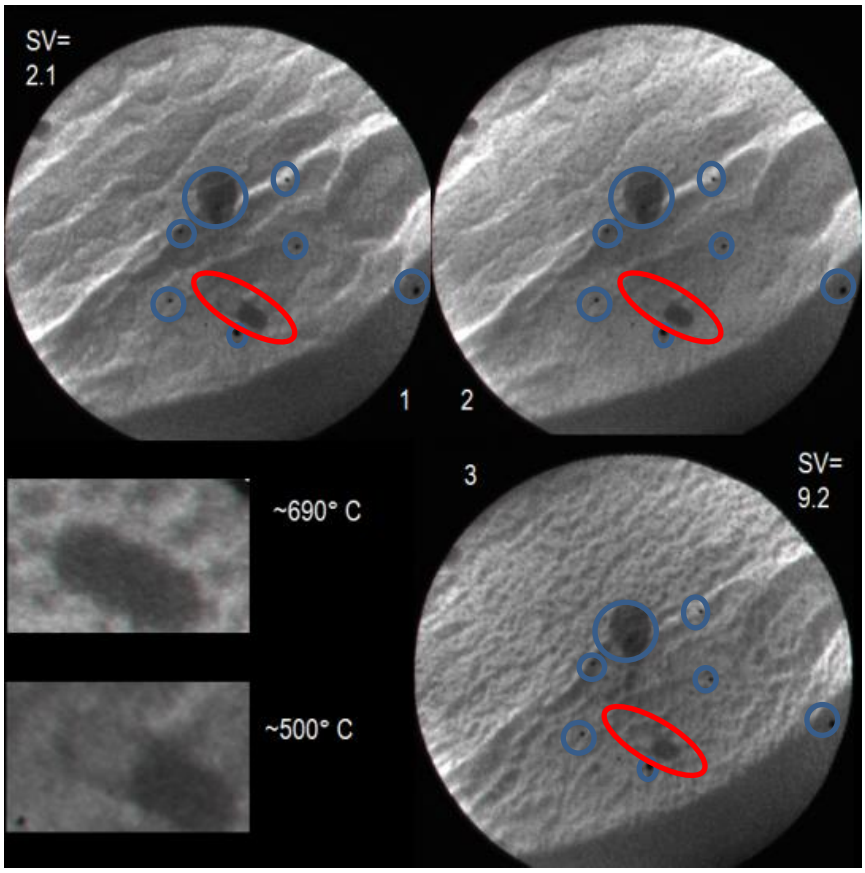

Figure 9: LEEM images of ~1 ML of Au at various start voltages (SV), shown in increasing order; 10 µm FOV; Images at the lower left are blown up images of a gold island before and after cooling from 690° C -500° C. This comparison shows the island collecting to the right side while cooling; Channel plate defects are circled in blue while gold islands are circled in red.

After the sample was cooled to just above room temperature, we investigated the surface structure using LEED (Fig. 10). We varied the start

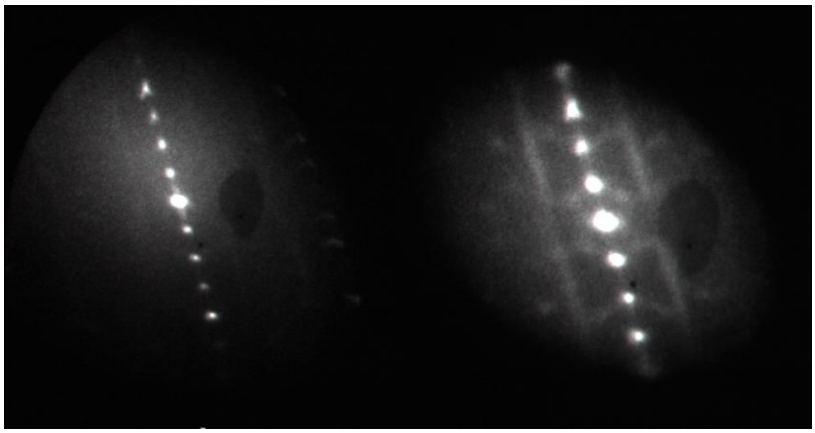

Figure 10: LEED images of 1 ML Au deposited at 690° C and cooled to room temperature . The left image is at SV = 6.6 V and the right image is at SV = 4.7 V.

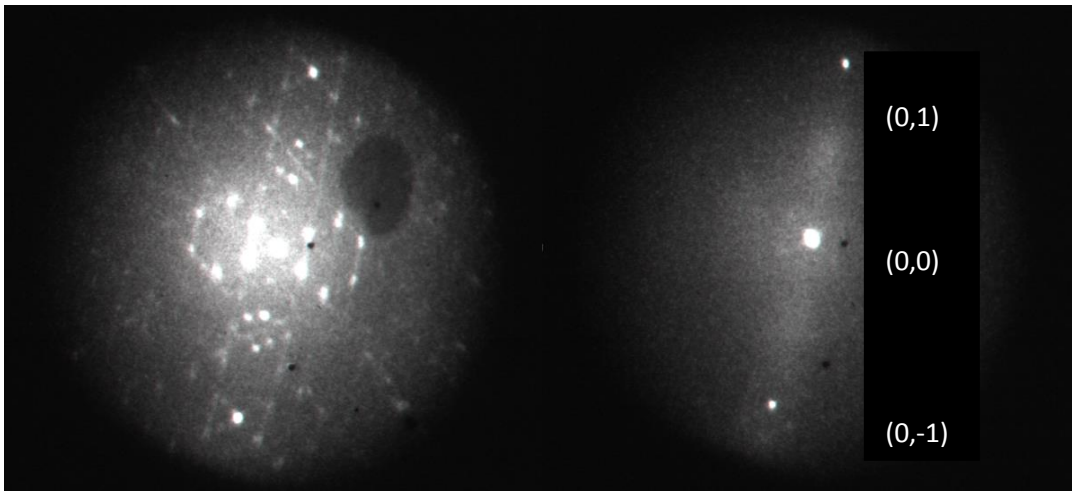

Figure 11: LEED images before (left) and after (right) a 0.5 ML dose

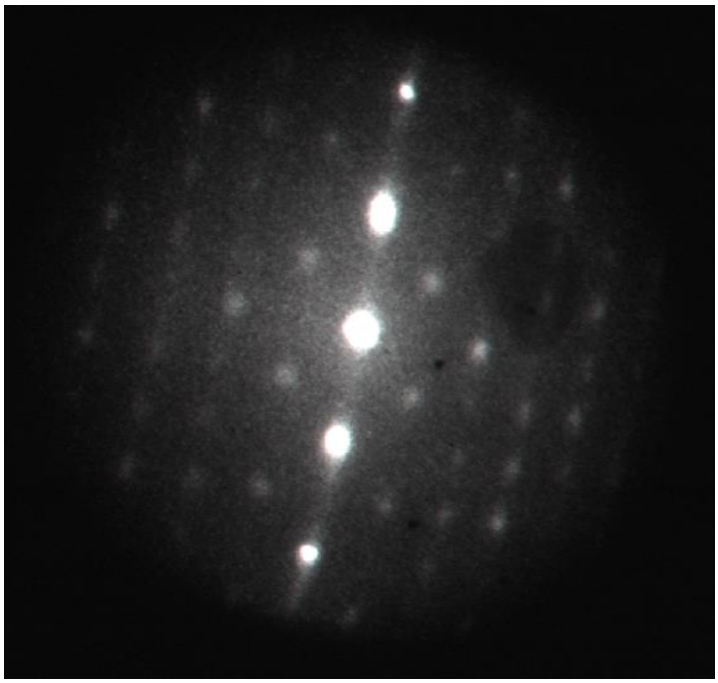

Figure 12: LEED image of the 0.5 ML surface reconstructing at ~450° C into a 4 x 4 phase

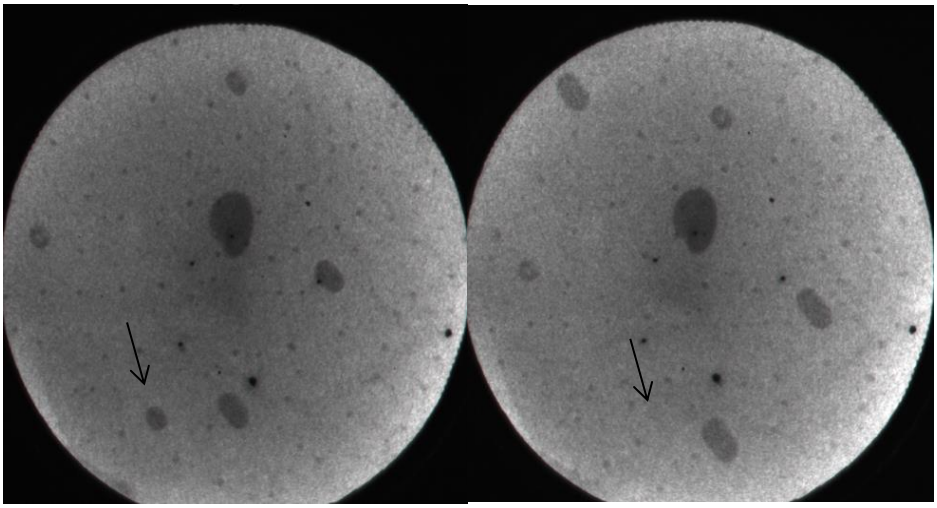

Figure 13: Before and after LEEM images of an island disappearing while the 0.5 ML surface was heated from 700° C - 750° C; 10 µm FOV

voltage and found that at SV= 4.7 V, the clean Ge LEED pattern of superimposed (16 x 2) and c(8x10) phases is faintly visible. At SV= 6.6 V and higher, the Ge pattern is no longer visible. Once gold is deposited, the LEED pattern that is visible, consists of three diffraction spots between the (0,0) and (0,1) spots, and the (0,0) and (0,-1) spots. The diffraction spots are arranged in columns.

Figure 11 shows images before and after 0.5 ML of Au is deposited onto clean Ge; the superimposed image of the (16 x 2) and c(8x10) phases disappears as the gold accumulates on the surface. What remains are the (0,0), (0,1), and (0,-1) diffraction spots that are a result of the bulk structure of Germanium. The gold on top caused the surface to reconstruct to a much less ordered state.

As we heated the sample to ~450° C we found that the surface reconstructed to a new phase which has a unit cell 4 times the size of germanium's bulk unit cell. It appears to be a (4 x 4) phase (Fig. 12). Heating the surface to just above the structural phase transition temperature caused the (4 x 4) pattern to disappear. When we cooled it back down, the pattern returned. This proves that the

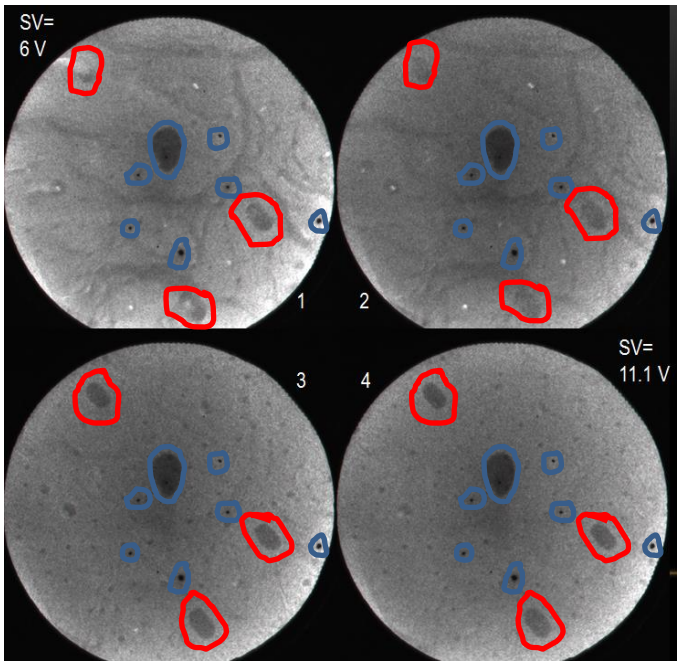

Figure 14: LEEM images of Au islands at various start voltages; shown in order of increasing starting voltage; 10 µm FOV; 750° C; Channel plate defect outlined in blue, islands in red

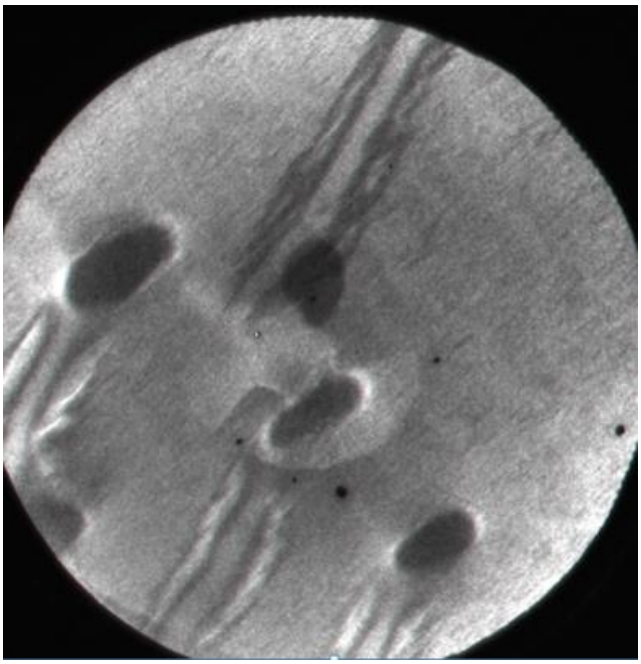

Figure 15: LEEM images of Au islands that remained on the surface after overnight sputtering and annealing; 20 µm FOV; room temperature

(4 x 4) reconstruction has a reversible phase transition. More work should be done to study this phase transition which exists only for a narrow range of temperatures. The temperature range should be measured more precisely.

As the sample is heated from 700° C to 750° C, we witnessed a small island shrink so much it was no longer visible (Fig. 13). A neighboring island about 1.5 µm away, grew slightly larger as the smaller island shrank. This is likely an example of Ostwald ripening, a phenomenon that describes the natural tendency of smaller particles to break up into even smaller pieces and redistribute on larger particles. The mass transport occurs because the larger islands are more energetically stable. Larger islands have a smaller percentage of surface atoms, which are less stable than interior atoms with more chemical bonds. We found that imaging with the SV turned down to 6 V caused bright spots to appear on Au islands

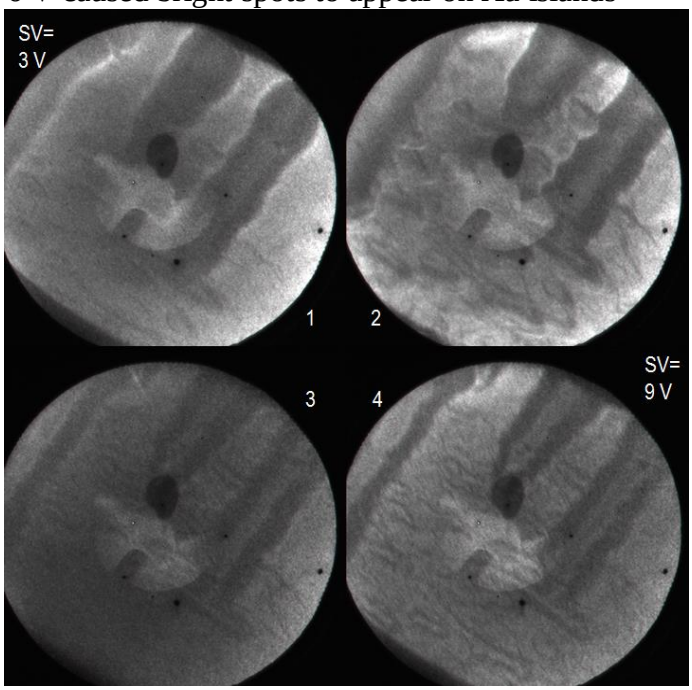

Figure 16: LEEM images of the left over Au islands at 650° C; 20 µm FOV

(Fig. 14). Lower start voltages revealed step bunches. At higher start voltages, the bright spots and step bunches disappeared. At SV = 11.1 V, tiny dark spots are visible and the bigger islands have a sharper border.

We found interesting structures as a result of overnight sputtering and annealing. The gold we deposited the previous day was not removed by the argon ion sputtering gun. At room

temperature, the islands were shaped like a stretched out V with oval islands at the tip, oriented in a common direction (Fig. 15). As we heated these structures to around 650° C, the long V shaped structure became wider as the gold spread out (Fig.16). At SV = 3 V, the outline of the structure is glowing bright, and what used to look like a V now looks more like an oval. Micro-scale craters are visible as the SV is increased and at SV = 9 V, steps are visible and the thicker stretched out V shape is visible. Next we cooled the sample down to room temperature. We adjusted the FOV to 10 µm and the result of heating and cooling the long V shaped structures was a large oval that was darkest along the border of the longest sides (Fig. 17). Many steps are visible around this gold structure. We dosed ~1.5 ML at 660° C, and the Au islands grew in two dimensions instead of just in one (Fig. 18). They were still oriented in a common direction as they grew, but they were much more circular. It seems that increasing the temperature during dosing makes the Au islands grow more preferentially in one direction. As we heated the sample to around 750° C the large islands with an average radius around 1 µm began moving in the direction along which the ovals were oriented (Fig. 19). Their longest side runs parallel to the direction the islands began moving. It seems that there was a critical size and

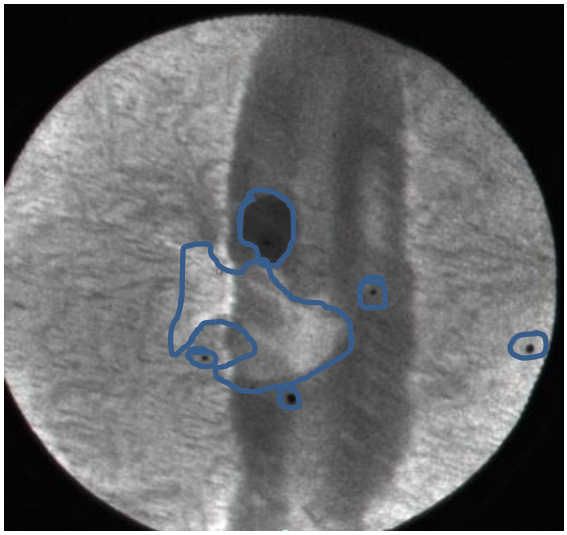

Figure 17: LEEM image of left over islands after being heated to 650° C and cooled back to room temperature; 10 µm FOV; Channel plate defects are outlined in blue

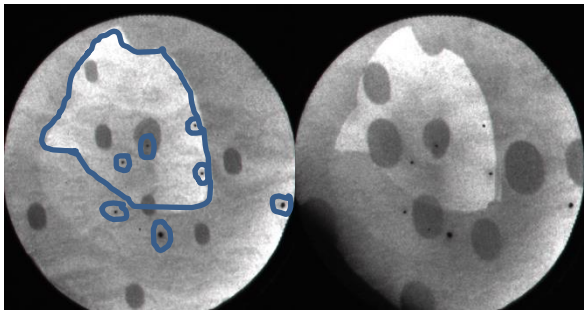

Figure 18: LEEM images of Au islands growing during (left) and after (right) dosing 1.5 ML at 660° C; 10 µm FOV; Channel plate defects are shown on the left, outlined in blue

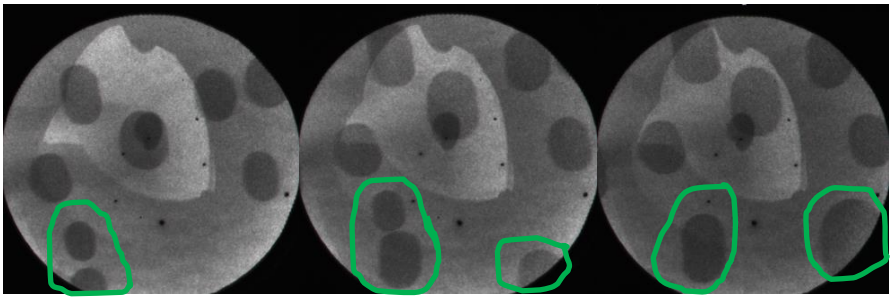

Figure 19: LEEM images shown in sequential order of two Au islands combining after the 1.5 ML dose. The islands outlined in green, began moving as sample was heated to 750° C; 10 µm FOV

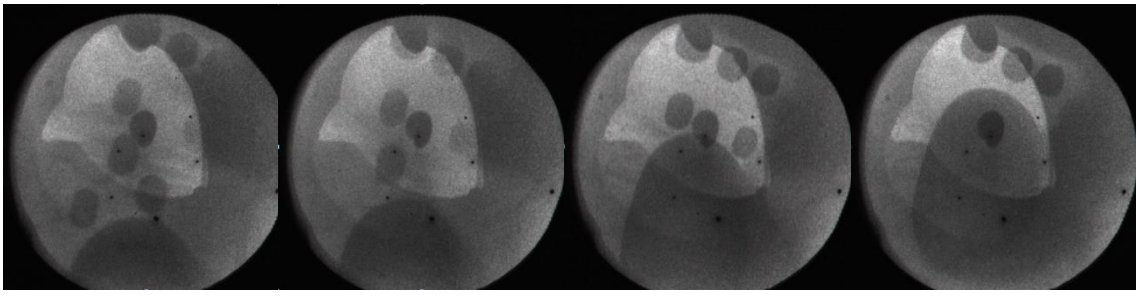

Figure 20: LEEM images shown in sequential order of a giant Au island moving across the surface, absorbing smaller islands in its path; 10 µm FOV

critical temperature for island diffusion to occur. As the sample continued to heat up to 760° C the mobile island keeps absorbing smaller islands in its path. As the temperature increased the islands moved faster. Immediately before absorption, when the large moving island approaches a *stationary island in its path (distance of about 0.1 μm)* the islands stretch towards each other due to a strong attractive force. It seems that when two islands interact, they will start to deform at a greater distance

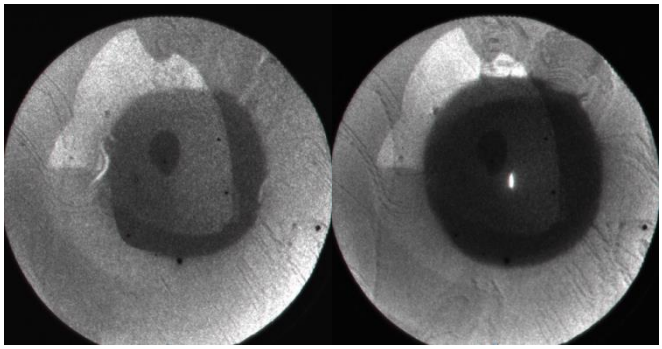

Figure 21: LEEM images of a large Au island which stopped moving after the sample was cooled to ~550° C. The left image is a lower SV while the right is a higher SV; 10 μm FOV

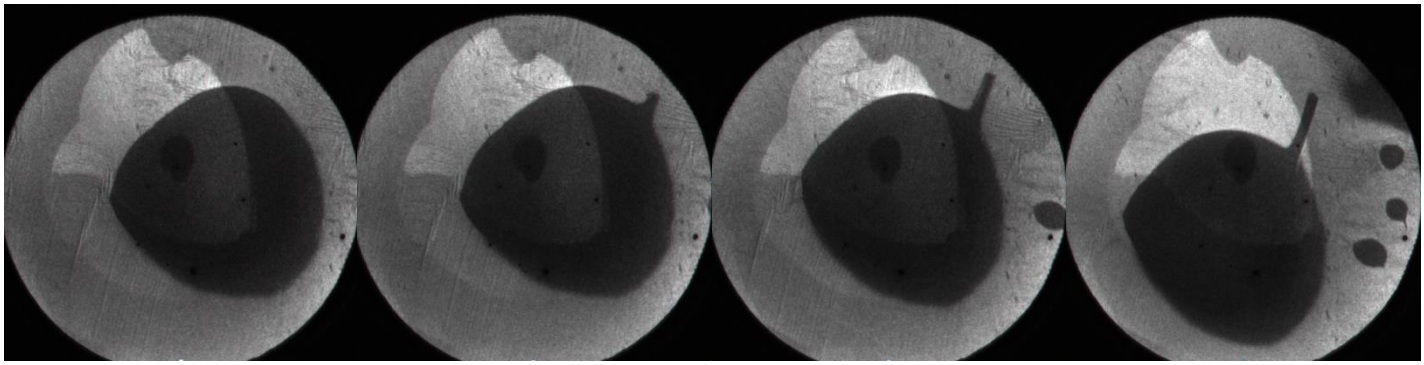

Figure 22: LEEM images shown in sequential order of a large Au island growing a rectangular formation as a result of heating the sample slowly to 400° C; 10 μm FOV

apart if they are bigger islands. Many more large moving islands are seen absorbing stationary islands as well as interacting with other mobile islands. As we cooled down the sample, the large moving island came to a stop at around 550° C (Fig. 21). Imaging in LEEM while adjusting the SV revealed a bright spot in the center of the massive island at lower start voltages. The sample was cooled to room temperature and then slowly heated to 400° C. As it was slowly heating, a rectangular formation suddenly grew off of the edge of the island (Fig. 22). The structure grew along steps and had long parallel sides that seemed to be contained between steps. Higher start voltages showed step details around the island, while lower start voltages revealed a very straight edge on what we thought was an oval shaped island (Fig. 23). Once we cooled the sample back to room temperature and observed the gold islands, we found that high start voltages (~18 V) revealed very complex structures on top of the gold island (Fig. 24). This was the only time we saw a lot of constructive interference on top of gold islands for the central (0,0) beam. We have seen only bright spots on top of islands in previous experiments.

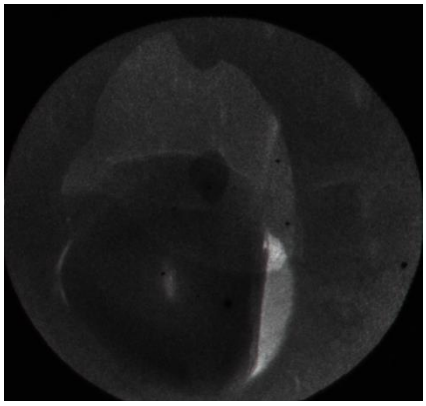

Figure 23: LEEM image of a large Au island; Low SV reveals the true shape of island on right side; 10 μm FOV

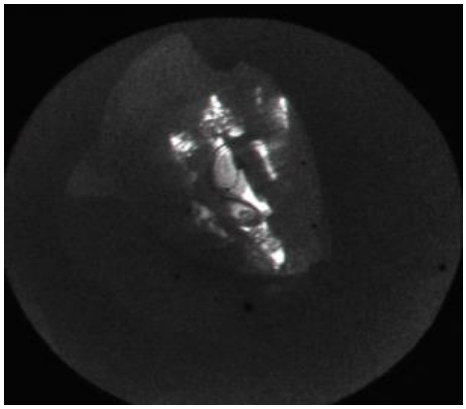

Figure 24: LEEM image of a large Au island at room temperature revealing bright and complex features; 10 μm FOV

Conclusions:

We used low energy electron microscopy and diffraction to study both, the clean Ge(110) surface and the growth of Au on Ge(110). Many interesting structures were found for various doses and temperatures. Au island growth on the Ge surface forms large islands that grow preferentially along the [1, -1, 0] crystallographic direction as temperature increases, and then collapses back into large circular islands when temperature decreases. The directional growth behavior has similarities to earlier observations of the Ag/Ge(110) growth mechanism although the lateral dimensions of the islands are quite different. A surface phase transition was discovered around 450° C. Large scale island diffusion was found to take place at around 750° C. Further research will be conducted on the growth mechanism of metals deposited on semiconductors at a variety of temperatures, as well as the collective behavior of the large number of atoms in these islands as they move across the surface. More research may lead to more exciting phenomena that may be beneficial in future attempts to build nanostructures on the surface of semiconductors. Applications for such nanostructures include chemical sensors, spintronic devices, and solar cells.

References:

- C. L. H. Devlin, D. N. Futaba, A. Loui, J. D. Shine, and S. Chiang, Mat Sci Eng. B96, 215-220 (2002).
- E. Bauer, M. Mundschau, and W. Swiech, Journal of Vaccuum Sci. and Tech. B9.2 (1991).
- Cory Mullet, PhD Dissertation, University of California, Davis (2012).
- Mullet, Cory H. *Growth of Ir on Ge(111) and Ge(110) and Growth of Ag on Ge(111), Ge(110), and Ge(001) Studied by Low Energy Electron Microscopy and Scanning Tunneling Microscopy.* UC Davis, 2012

Figures:

1) Devlin et al. "A unique facility for surface microscopy." *Materials Science and Engineering.* B96. (2002): 215-230. Print.
2) Marshall Van Zijll, PhD. Dissertation, University of California, Davis (2014).
3) A. Loui, PhD Dissertation, University of California, Davis (2005).
4) J. A. Giacomo, PhD Dissertation, University of California, Davis (2009).
5) Ichikawa et al. Sol. St. Commun. 93, 541 (1995).
   Ichikawa, Surf. Sci. **560**, 205 (2004).
   Ichikawa, Surf. Sci, **560**, 213 (2004).
6) Cory Mullet, PhD. Dissertation, University of California, Davis (2012).

8a) Cory Mullet, PhD. Dissertation, University of California, Davis (2012).